COLLAPSE BEHAVIOUR OF THIN-WALLED CFRP STRUCTURES DUE TO MATERIAL AND GEOMETRIC NONLINEARITIES – EXPERIMENTS AND SIMULATION

Richard Degenhardt*, Jan Tessmer*, Alexander Kling*

***DLR, Institute of Composite Structures and Adaptive Systems, Lilienthalplatz 7, 38108 Braunschweig, Germany**

Keywords: *Collapse, Composites, Experiments, Simulation, Validation*

Abstract

Aerospace industry strives for significantly reduced development and operating costs. Reduction of structural weight at safe design is one possibility to reach this objective. Another one is the use of reliable simulation methods in order to minimize expensive and time consuming experimental design studies. DLR has developed improved concepts and tools for fast and reliable simulation of the buckling and the postbuckling behaviour of thin-walled structures up to collapse, respectively, which allow the exploitation of considerable reserves in primary fibre composite structures in aerospace applications [1-4]. For the validation of these concepts and tools, a sound database of experiments is needed. Such has grown considerably through many recent projects (e.g. EU-"COCOMAT" [5,6], EU-"POSICOSS", ESA-"Probabilistic Aspects of Buckling Knock Down Factors — Tests and Analysis", etc.). The paper presents first the experimental activities at the buckling test facility of the DLR Institute of Composite Structures and Adaptive Systems with an overview about buckling, postbuckling and collapse tests in combination with advanced measurement systems. Secondly, suitable computational methods are presented.

1 Introduction

European aerospace industry strives for reduced development and operating costs, by 20% and 50% in the short and long term, respectively. One possibility to reach this objective is to reduce structural weight at safe design. The Institute of Composite Structures and Adaptive Systems (DLR) contributes to this aim within several research activities presented in this paper. For more than 40 years already this institute is actively involved in solving problems of buckling and postbuckling of thin shell structures. An eminent aspect of its scientific work in this field is the close interaction between theoretical effort and experiments. Through the continuous involvement in performing buckling tests considerable experience and acknowledged expertise has been accumulated and is used in the EU project *COCOMAT* and the ESA study *Probabilistic Aspects of Buckling Knock Down Factors – Tests and Analysis*.

The project COCOMAT that comprises knowledge and skills from 15 European partners and which is co-ordinated by DLR, started in January 2004 and ends October 2008. COCOMAT is the acronym of *Improved MATerial Exploitation at Safe Design of COmposite Airframe Structures by Accurate Simulation of Collapse*. The COCOMAT project builds up on the finished EU project POSICOSS which developed fast tools for the postbuckling analysis of fibre composite stiffened panels, created experimental data bases and derived design guidelines. COCOMAT [5, 6] goes beyond the POSICOSS results by simulation of collapse. There is a need to find out, how deep into the postbuckling regime the loading can be extended without severely damaging the structure, and how the behaviour can be predicted by fast and precise simulation procedures. In that sense COCOMAT improves existing tools for design and analysis, sets up design guidelines suitable for stiffened panels taking skin stringer separation and material degradation into account, and it creates a comprehensive experimental data base concerning such structural components. The whole project considers 7 different designs within 47 tests. DLR considers 2 of the designs which are manufactured 12 times in total for testing under different conditions (undamaged, pre-damaged, static loading, cyclic loading).

The ESA study *Probabilistic Aspects of Buckling Knock Down Factors – Tests and Analysis* started in May 2006 and ended December 2007. The main objectives of this study are to achieve an improved buckling knock-down factor (the ratio of buckling loads of imperfect and perfect structures) for unstiffened CFRP cylindrical shells and to validate the linear and non-linear buckling simulations by test results. In the NASA SP-8007 design guideline from 1968 a lower bound curve for the knock-down factor is proposed. This factor is relatively conservative and the structural behaviour of composite material is not considered adequately. Advanced thin-walled cylindrical shell structures under compression are therefore penalized if the knock-down factor based on this early NASA report must be applied. The main results of the ESA study comprise an experimental data base of 10 nominally equal axially compressed CFRP cylinders, sensitivity analyses using Monte-Carlo simulation, validation with tests and a design guideline for that type of structure with a less conservative knock-down factor than taken from NASA SP-8007 [11].

For the validation of all concepts and tools a great number of experiments are needed which were also performed within these projects. This paper focuses on the one hand on the experimental activities of the projects performed at the buckling test facility at DLR. It explains the working of the buckling test facility, the advanced measurement systems, which are running in parallel to the tests, and gives exemplarily some test results. On the other hand, suitable computational methods are presented. The structures considered are unstiffened cylinders as well as panels stiffened by stringers. The unstiffened cylinders (ESA study) are more related to space applications (e.g. Ariane busters or parts of the int. space station ISS) and the stiffened panels (COCOMAT) focus more on aircraft structures (e.g. fuselage).

Attention has to be drawn to the fact of distinguishing between industrial structures and validation structures. The validation structures are designed as to specific limiting aspects of application of the software to be validated [15, 16] (e.g. large postbuckling region with an early onset of degradation). Industrial structures are designed regarding to industrial needs, where the performance of the structure itself is in the foreground.

The load case considered for all investigations presented in this paper is axial compression under static loading. However, it must be mentioned that the DLR buckling test facility has the capability to test structures also under internal pressure and torsion by static loading as well as axial compression under dynamic loading. The structures may be subjected to separate as well as to combined loading modes.

2 Definitions

The terms *buckling*, *postbuckling* and *collapse* and are explained in the following based on experimental results of a stiffened panel. Figure 1 illustrates a realistic (experimentally measured) load-shortening curve of an axially compressed stiffened CFRP panel tested at the DLR buckling test facility representing a stringer dominant design.

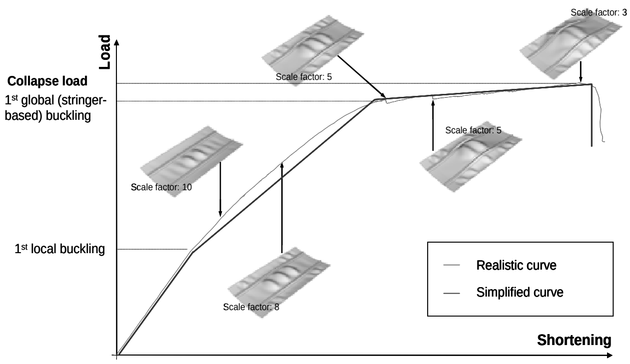

Fig. 1. Load-shortening curve of an axially compressed stiffened CFRP panel

It explains the terminology of three remarkable load levels. The lowest one usually provokes the first local buckling where the buckling mode is restricted to local skin buckles between the stringers. The second level causes the first global buckling which is stringer based-buckling. The highest load level is reached at collapse. The other curve is a simplified representation of the real load-shortening curve with knees at these characteristic load levels.

First local buckling: This is the onset of buckling of the skin between the stiffeners. It is represented by several small local buckles and occurs in stiffened aerospace structures usually as the first buckling mode (before first global buckling). At this point there is a slight knee in the load-shortening curve and the axial stiffness is slightly decreased.

First global buckling: This is the onset of buckling of the stiffeners. It is represented by a global buckle of the structure and also a larger knee in the load-shortening curve. Typical aerospace structures are usually stringer dominant and show here a larger decrease of the axial stiffness. For these kinds of structures the first global buckling load is usually beyond the first local buckling load.

Collapse: Collapse is specified by that point of the load-displacement-curve where a sharp load decrease occurs. This is usually the maximum value of the load carrying capacity.

Postbuckling: The area between the first buckling load (usually first local buckling) and the collapse load is called postbuckling area.

For *unstiffened cylinders* the definitions are in principal the same. However, one does not distinguish between local and global first buckling because there are no stiffeners. The *first buckling* can be characterized by some local buckles or by buckles distributed around the cylinder, depending on homogeneity of load introduction and test structure. After first buckling there is usually a significant decrease of the load in the load-shortening curve. *Collapse* is marked by the maximum load value of the load-shortening curve, and the *postbuckling* area is that after first buckling.

3 DLR buckling test facility

Figure 2 shows a photo of the buckling test facility of the DLR Institute of Composite Structures and Adaptive Systems. The test machine is mainly designed for high precision buckling tests of thin-walled shells like cylinders or panels under axial loading, torsion or internal pressure. The load history of axial compression ranges from static loading to shock loading. The hydraulic cylinder is equipped with a small servo-valve for static tests additionally with a second valve for high dynamics. Table 1 summarizes the characteristics of the test facility. More details to the test facility are given in [7].

Fig. 2. Buckling Test Facility at DLR

Table 1. Characteristics of the DLR buckling test facility

Load case	
Axial compression	Max. 1000 kN
Torsion	Max. 20 kNm
Internal pressure	Max. 800 kPa
External pressure	Max. 80 kPa
Geometry limits of the test structure	
Length	Max. 1600 mm
Width (diameter)	Max. 1200 mm
Load frequency	Max. 50 Hz

4 Preparation of the test structures

After the manufacturing process the preparation of the test-structure up to the test plays an important role to ensure reliable and high quality experimental data. In the following the preparation process performed is described. Some steps using advanced measurement systems as full scale thickness measurement or imperfection measurement may not be in all cases required if for instance imperfection sensitivity is not expected to play a major role.

- Ultrasonic inspection
- Thickness measurement
- Casting of the s into preliminary end boxes, hardening of the end blocks
- Detaching from the boxes
- Milling of the end block edges
- Measuring of the imperfection (ATOS)
- Application of longitudinal edge supports
- Application of strain gauges
- Stress free casting into final end boxes
- Connection of the strain gauges to cables
- Application of sensors for the Lamb-waves method (SHM)
- Assembling to the buckling test facility

5 Advanced measurement systems

Running stability tests is an expensive task. Further, testing the structures until collapse can be performed only once. In order to get as many results as possible (e.g. information about degradation of skin-stringer separation) already during the tests or even to perform a 360° full scale deformation measurement highly advanced measurement systems are applied before and during the tests.

5.1. Before the test

5.1.1 Non-Destructive Testing and thickness measurement

The automatic ultrasonic testing of CFRP structures using water split coupling is applied to detect any defects in the structure (e.g. delaminations). The same test method can be utilized for full field thickness measurement. The test is carried out with a broadband transducer in echo-technique and the results are displayed in a D-scan.

5.1.2 ATOS system- Optical measurement of imperfections

In order to identify the real shape of the skin of the test-structure, ATOS, an optical 3D digitizing measurement system (based on photogrammetry), is utilized to extract the actual radius of the panel as well as the initial geometric imperfections of the skin utilizing a best-fit procedure. Differences between the nominal and measured structure can for instances be due to snap-back effects during the manufacturing process.

5.2. During the test

During testing a mixture of conventional (e.g. strain gauges) and advanced measurement systems are applied. At the beginning, after calibration of the test set-up, the test-structure is loaded by three cycles up to about 50% of the expected linear buckling load in order to compensate possible settlements, followed by loading until the load level planned (e.g. collapse). The load and the respective shortening, the strains, the displacement field of the skin, single transverse displacements of the stringer blades are measured and video records are taken. The strains are measured by strain gauges at different positions and directions. The displacement field of the skin is gauged by the ARAMIS system, which is based on an optical 3D digitising method [7]. In order to measure the degradation of the skin-stringer connection the following three methods are applied (for details, see [7-9]):

- Lamb-waves
- optical lockin thermography
- High-Speed ARAMIS-system.

Figure 3 shows the position of the thermography equipment for the measurement from skin-side of the panel and the ARAMIS system for the measurement from stringer-side of the panel.

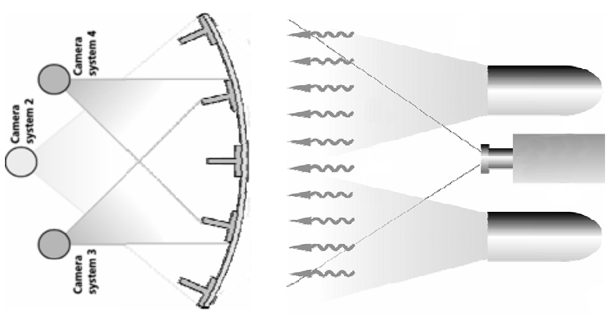

Fig. 3. Schematic drawing of the test setup (ARAMIS (left) and lockin thermography (right))

Figure 4 shows out-of-plane deformations of an stringer stiffened panel obtained by ARAMIS compared to numerical ABAQUS simulation. It demonstrates the advantages of the ARAMIS system to have a full scale measurement.

During testing load and shortening are measured as global values of the structural behaviour. Three load cells are located between drive plate and load distributor, the applied load is calculated as the sum of the three loads. Two displacement pickups are mounted between load distributor and top plate. The shortening is calculated as the average of the measured displacements. The pickups also serve for displacement control of the servo-hydraulic cylinder. So the deformations of the test facility, in particular of the load cells, are settled.

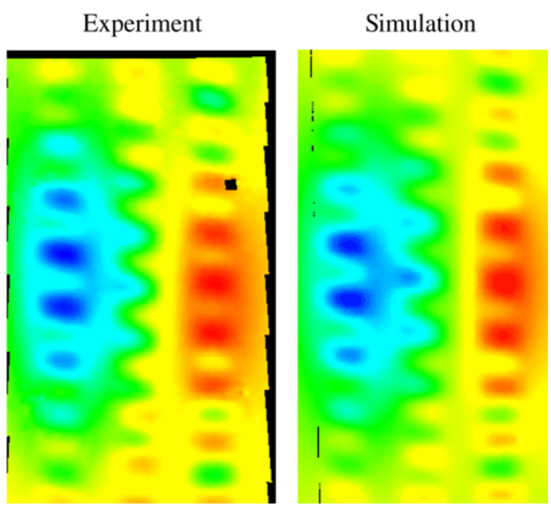

Fig. 4. Comparison of experiment and simulation in the deeper postbuckling regime

6 Material properties

Within the COCOMAT project and the ESA study DLR used the same prepreg material IM7/8552 (Hexcel). Although the properties for that kind of material are known from the producer, for each project an own test series on small specimens was performed in order to obtain real material properties used in the project and in order to have more information about the sensitivity and reliability of the material properties for the selected prepreg system. The testing methodology followed the procedure given in the German standard DIN 29971. Table 2 gives a summary of the test results for the stiffnesses and strength values with the corresponding standard deviations. The test procedure was in all cases under the same conditions, however, the material was manufactured by different partners. This is likely the reason for differences between the mean values or standard deviations.

Table 2. Material properties of CFRP prepreg IM7/8552 UD

	COCOMAT		**ESA study**	
	Mean value / Standard deviation			
Stiffness	(GPa)	(%)	(GPa)	(%)
$E_{t\,L}$	164.1	3.01	175.3	1.38
$E_{c\,L}$	142.5	1.69	157.4	2.39
$E_{t\,T}$	8.7	3.91	8.6	2.9
$E_{c\,T}$	9.7	4.85	10.1	4.11
$G_{L\,T}$	5.1	13.73	5.3	1.10
Poisson's ratio	-	(%)	-	(%)
$\nu_{L\,T\,(t)}$	0.28	14.44	-	
Strength	(N/mm2)	(%)	(N/mm2)	(%)
$R_{t\,L}$	1741	11.92	2440	3.54
$R_{c\,L}$	854.7	9.04	1332	7.24
$R_{t\,T}$	28.8	5.23	42	26,45
$R_{c\,T}$	282.5	18.16	269	5.95
$R_{L\,T}$	98.2	17.54	129	0.84

t = tension, c = compression
L = longitudinal direction, T = transverse direction

7 Test results

7.1. Cyclic tests and collapse test of a stiffened panel

The following test results were obtained on the panel P29 manufactured by AERONNOVA and tested by DLR. Panel P29 is one validation design which is not pre-damaged and which was axially loaded first 3800 times by cyclic loading and finally until collapse. Table 3 summarises the nominal and measured data of this panel.

Table 3. DLR panel P29: Nominal and measured data

Geometry / Lay-up	**Nominal**	**Measured**
Panel length	l = 780 mm	l = 780,5 mm
Free length (buckling length)	l_f = 660 mm	l_f = 660 mm
Radius	r = 1000 mm	r = 848 mm
Thickness	t =1 mm	t =0,98 mm
Arc length	a = 560 mm	a = 560,5 mm
Number of stringers	n = 5	n = 5
Distance stringer to stringer	d = 132 mm	d = 132 mm
Distance stringer to longitudinal edge	e = f /2 = 16 mm	e = 16.2 mm
Laminate set-up of skin	$[90, +45, -45, 0]_s$	
Laminate set-up of stringers	$[(+45, -45)_3, 0_6]_s$	
Blade: (cf. Fig. 5)	$[(45,-45)_3,0_6]$	
Flange:		
Ply thickness	t = 0.125 mm	
Stringer thickness	t = 3 mm	t = 2,9 mm
Stringer height	h = 14 mm	h = 14,3 mm
Stringer width	f = 32 mm	f = 32 mm
Panel mass, g		1238 g

The geometry of the stringer is illustrated in Figure 5.
Material properties are given in Table 2.

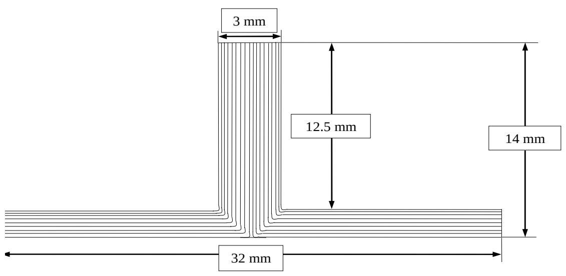

Fig. 5. DLR panel P29 - Stringer type

Before the test, the panel was investigated by ultrasonic inspection and ATOS – the optical measurement system determining best-fit radius and imperfection. During the test the panel was loaded statically and displacement-controlled by axial compression at 3 different load steps:

1) 2000 load cycles until the shortening of u = 1.08 mm (just beyond global buckling, 80% of expected collapse)
2) 1800 load cycles until the shortening of u = 1.93 mm (95% of expected collapse)
3) 1 step until collapse

Figure 6 illustrates the load-shortening curves after 2000 cycles and the final collapse test. The first 2000 cycles, which were loaded just beyond global buckling, did not show any indication for degradation. In the 2nd load step of the next 1800 cycles the skin-stringer separation started. After each 400th cycle the test was stopped and a thermography measurement was performed. Figure 7 illustrates the load-shortening curve and ARAMIS measurements at selected prints of the final collape test. Figure 8 shows measurements at cycle 3601 (u=2.0 mm) and after collapse. The separated areas of skin and stringers are clearly visible. More details are presented in [7, 10].

7.2 Buckling tests of unstiffened cylinders

Within the ESA study, tests of the 10 nominally equal cylinders were performed (cf. Table 4). Before testing, ultrasonic inspections assured the absence of major inhomogeneities in the laminate and provided information on the thickness distribution. Next, the cylinders were inspected by the ATOS system to measure the shape imperfections. During the test the cylinders were loaded by axial compression just beyond the buckling load. In that loading area the structure behaves elastically and will not be damaged. The full scale deformations and buckling shapes were measured using the ARAMIS-system.

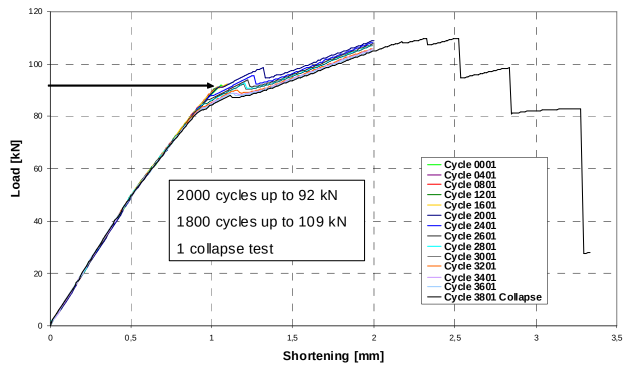

Fig. 6. DLR panel P29 – Test results (cyclic loading)

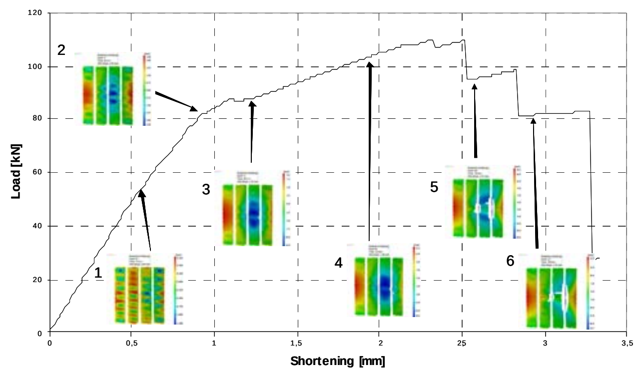

Fig. 7. DLR panel P29 – Test results (Final collapse test)

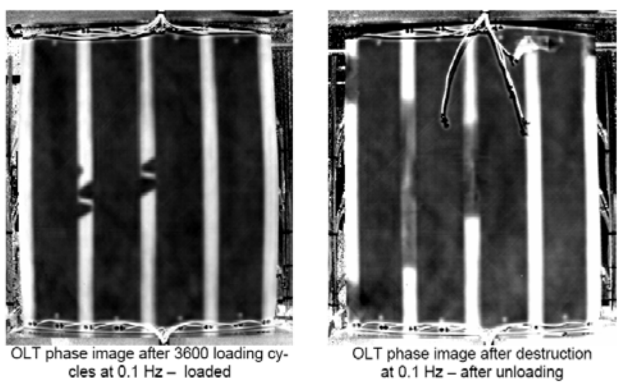

Fig. 8. Panel P29: OLT measurement at cycle 3601 (u = 2.0 mm) and after collapse (u=3.3mm)

Figure 9 illustrates the measured load-shortening curves of all tests with 3 selected ARAMIS measurement pictures obtained from the 360° measurement of cylinder Z15U500. Picture A and B are from the pre-buckling and Picture C from the early postbuckling region. Picture B is just before and Picture C just after the first buckling load.

Table 4. DLR Cylinders: Nominal and measured data

Geometry / Lay-up	Nominal	Measured (cylinder Z15U500)
Total length	l = 530 mm	l = 530 mm
Free length (buckling length)	l_f = 510 mm	l_f = 510 mm
Radius	r = 250 mm	r = 248,5 mm
Thickness	t = 0.5 mm	t = 0.51 mm
Lay-up	+24,-24,+41,-41	
Cylinder mass, g		638 g

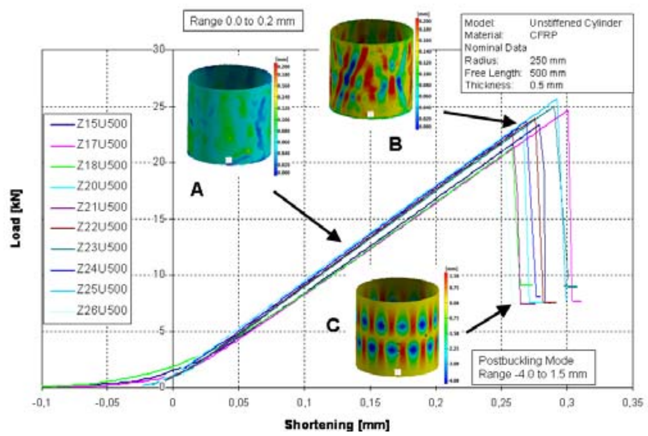

Fig. 9. Load shortening curves of 10 tested cylinders and ARAMIS measurement of Z15U500

Table 5. DLR Cylinders: Test results

Cylinder	Buckling load [kN]	Shortening at buckling [mm]	Axial stiffness [kN/mm]
Z15U500	23.36	0.279	83.61
Z17U500	24.63	0.301	81.82
Z18U500	21.32	0.258	81.89
Z20U500	23.08	0.266	84.67
Z21U500	22.63	0.259	86.23
Z22U500	23.99	0.276	84.82
Z23U500	25.02	0.290	84.51
Z24U500	23.62	0.269	85.05
Z25U500	25.69	0.293	84.34
Z26U500	22.43	0.252	84.99

Table 5 summarizes main results from the buckling tests. The buckling loads range between 21.32 kN and 25.69 kN. It shows also the shortening at buckling and the axial stiffness. More details are given in [11].

8 Simulation

8.1. ABAQUS simulation of stiffened panels

For simulation the skin-stringer separation of composite structures DLR developed an ABAQUS user subroutine, which uses stress-based failure criteria for the degradation of the adhesive. This software was applied to calculate the collapse behaviour of Panel 23. This panel is nominally the same design as Panel 29, however, it was loaded directly in one load step until collapse. A comparison of test and simulation is therefore easier. Figure 10 shows the comparison of the load shortening curves of the simulation with test results. It can be seen that the calculations which do not take degradation into account are very good until the global buckling. Beyond that point there is a discrepancy because skin-stringer separation is not considered. The improved ABAQUS simulation with the user-subroutines shows a good agreement even after global buckling. However, within the simulation more adhesive elements failed than in the test. Detailed results can be found in [12].

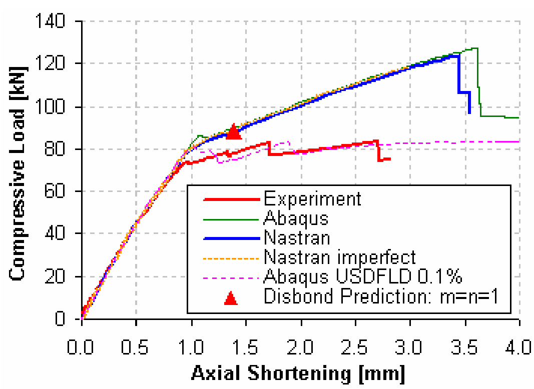

Fig. 10. Comparison of test and simulation [12]

8.2. Simulation of unstiffened cylinders

For the early design phase fast calculation methods are needed. For this purpose Geier and Singh [13] developed a method to calculate the buckling load semi-analytically based on the shallow shell theory. By means of this approach combined with a knock-down factor, which covers the effect of imperfections, a fast method for designing an axially compressed cylindrical CFRP shell is available. Unfortunately, the knock-down factor has still to be taken from the conservative NASA SP-8007 design guideline, which does not take any information about the lay-up into account. To determine an improved knock-down factor by FE simulation, an accurate description of all imperfections is required. In this section, ABAQUS simulations with deterministically considered thickness and geometric imperfections are presented and compared to test results.

To choose the most effective numerical analysis, several static solvers available in ABAQUS/Standard (linear buckling analysis, Newton Raphson Method, Newton Raphson Method with artificial damping (Stabilize method), Riks (Arc-length), Newton Raphson Method with continuously parallel running linear buckling analyses, Newton Raphson Method with a dynamic analysis restart) and a dynamic analysis with ABAQUS/Explicit were applied. For convergence studies different mesh refinements (between 675 and 97,200 elements) were used. The result of these investigations led to a FE-Model with about 12,000 elements and the Newton Raphson Method with artificial damping as solver. In addition, 2000 elements are used to model the test boundary condition as closely as possible (clamped in a ring of resin) with 3D-elements.

By choosing an imperfection sensitive cylinder design every kind of imperfection or boundary conditions has a strong influence on its buckling behaviour, cf. Figure 11. That is why the buckling load of the simulation with the perfect cylinder (38.2 kN) diverges significantly from the buckling test (e.g. 22.43 kN for cylinder Z26). However, with each infliction of imperfection in the FE-analysis the buckling load gets closer to the test result. The curves show the influences of the geometric imperfection and the variation in the thickness. With an in-house tool the thickness scan can be introduced in the FE-model. This lowers the buckling load from 38.2 kN of the peferct cylinder down to 36.3 kN. Another tool includes the geometric imperfection, measured with the ATOS system, into the model. This imperfection lowers the buckling load to 32.8 kN. Both imperfections together push the buckling load down to 31.2 kN. Still, the experimental buckling load of 22.43 kN is not yet reached. The difference may be caused by further imperfections like material inhomogeneities or load imperfections.

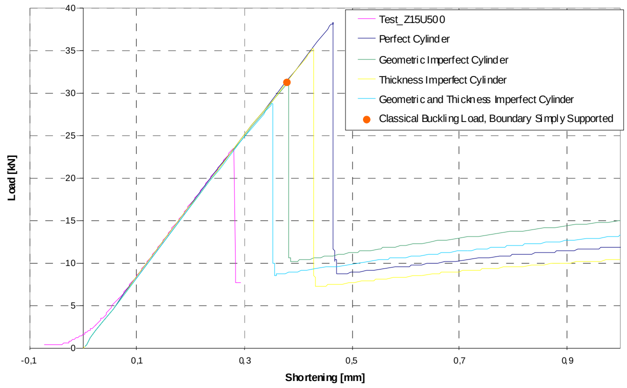

Fig. 11. Load-shortening curves, comparison test and simulation

The classical buckling load, which will be the basis for the determination of the knock-down factor, is given as a small dot. The value (31.3 kN) is located between the buckling load for the perfect cylinder and the test result. In contrast to the FE simulation the calculation of the classical buckling load does not restrain warping along the edges. Consequently, the classical buckling load is smaller than the FE buckling load of the perfect cylinder. However, this effect is outweighed by the influence of all possible imperfections. Further details are given in [11].

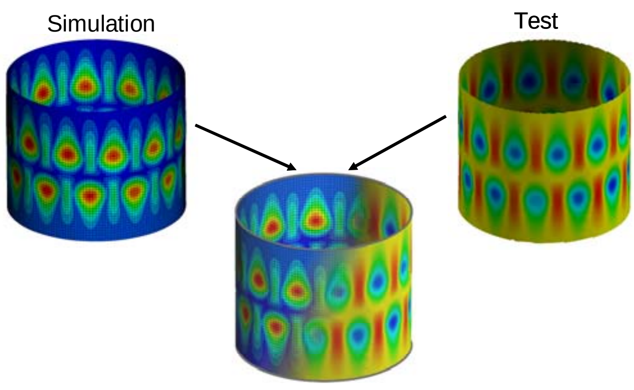

Fig. 12. Postbuckling pattern, comparison test and simulation

Figure 12 compares the post-buckling pattern between the test and simulation. The left picture is obtained by the 360° ARAMIS measurement and agrees quite well with the simulation in the right figure. This buckling behaviour was observed for 10 tested cylinders.

8.3. IBUCK-Fast simulation tool for stiffened aerospace panels

The fast tool iBuck, recently developed by DLR, may be used to assess to post-buckling behaviour of bi-axially stiffened cylindrical shells under axial or transverse load, in-plane or lateral pressure [14]. In addition, the loading by an external bending moment may be considered. The panels are assumed to be representative for a fuselage section and are comprised of a skin (shell) and stiffeners in both longitudinal (stringers) and circumferential direction (frames). In addition, aircraft-specific components such as doublers (used to reinforce the skin underneath the stiffeners) and clips (providing lateral support for the frames) are included in the model. Stringers and frames are considered as structural elements with independent degrees of freedom, where continuity in terms of rotation at the interface skin/stiffeners and in terms of end-shortening is enforced. Local and global buckling modes are superimposed. Local buckling is defined as skin buckling and skin-induced stiffener rotation within a bay. During local buckling, the stiffeners themselves are not allowed to deflect in out-of-plane direction. During global buckling, that is, buckling across several bays, the stringers may deflect in out-of-plane direction, whereas the frames, being much heavier than the stringers, are fixed in out-of-plane direction.

IBUCK is a semi-analytical tool, which means that the problem formulation is based on the foundations of analytical continuum mechanics and that numerical methods are used to discretize the problem and to solve the resulting equations. The potential energy of the structure is computed, taking finite deflections and thus non-linear strain-displacement relations of skin and stiffeners into account. At each load step, stationary values of the potential are sought. The resulting set of third-order equations is discretized using a Ritz approach, that is, by selecting appropriate deflection functions for the skin and the stiffeners. The equations are solved by applying incremental perturbation theory in the form of an arc-length method.

The comparison of IBUCK with an ABAQUS FEM calculation is given in Figure 13. Figure 14 illustrates one postbuckling pattern obtained by IBUCK. Currently, IBUCK is under extension for consideration of composite structures. More details are given in [14].

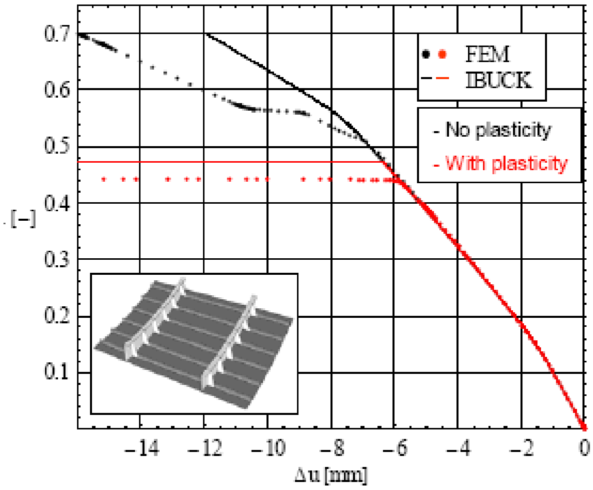

Fig. 13. Comparison of iBUCK and FEM [14]

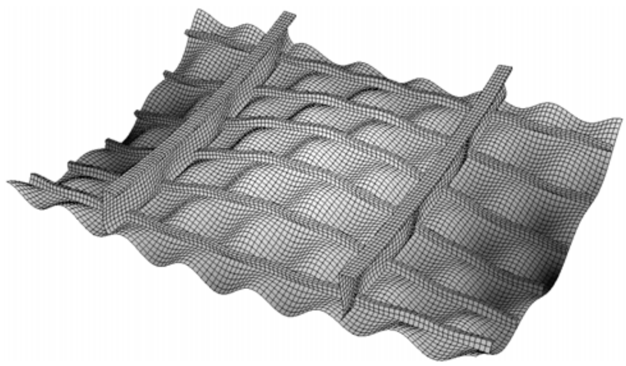

Fig. 14. Postbuckling shape obtained by iBUCK [14]

9 Summary

The paper presents experimental and numerical investigations of the buckling and collapse behaviour composite structures obtained by the DLR Institute of Composite Structures and

Adaptive Systems. Structures considered are stiffened panels with application in the aerospace and unstiffened cylinders which are more space related. Test results, numerical investigations and a comparison of test and simulation are given.

10 Acknowledgements

The project *COCOMAT* was supported by the European Commission. The study *Probabilistic Aspects of Buckling Knock Down Factors* was funded by the European Space Agency (ESA). All support is gratefully acknowledged. The information in this paper is provided as is and no warranty is given that the information is fit for any particular purpose. The reader thereof uses the information at its sole risk and liability.

References

[1] Degenhardt R, Kling A and Rohwer K. Design and analysis of stiffened composite panels including post-buckling and collapse. *Computers and Structures*, Vol. 86, pp 919-929, 2008.

[2] Degenhardt R and Tessmer J. New Achievements in Stability of Composite Airframe Structures. *Proceedings of the 12th Australian International Aerospace Congress*, Melbourne, Australia, 19-22 March, 2007.

[3] Degenhardt R and Tessmer J. Improved Design Scenario for Composite Airframe Structures. *Proceedings of the 48th AIAA Conference on Structures, Structural Dynamics and Materials*, Hawaii, USA, 23-26 April, 2007.

[4] Zimmermann R, Klein H and Kling A. Buckling and postbuckling of stringer stiffened fibre composite curved panels — Tests and computations. *Compos. Struct.*, Vol. 73, pp 150–161,2006.

[5] www.cocomat.de

[6] Degenhardt R, Rolfes R, Zimmermann R and Rohwer K. COCOMAT - Improved MATerial Exploitation at Safe Design of COmposite Airframe Structures by Accurate Simulation of Collapse. *Composite Structures*, Vol. 73, pp 175-178,2006.

[7] Degenhardt R, Kling A, Klein H, Hillger W, Goetting HC, Zimmermann R and Rohwer K. Experiments on Buckling and postbuckling of Thin-Walled CFRP Structures using Advanced Measurement Systems. *International Journal of Structural Stability and Dynamics*, Vol. 7, No.2, pp 337–358,2007.

[8] Hillger W and Pfeiffer U. Structural Health Monitoring Using Lamb Waves. *9th European Conference on Non Destructive Testing*, Berlin, Germany, 2006.

[9] Busse G, Wu D and Karpen W. Thermal wave imaging with phase sensitive modulated thermography. *J. Appl. Phys.*, Vol. 71, No. 8, pp 3962–3965, 1992.

[10] Degenhardt R, Wilckens D, Klein H, Kling A, Hillger W, Goetting HC, Rohwer K and Gleiter A. Experiments to detect the damage progress of axially compressed CFRP panels under cyclic loading. Special volume of *Key Engineering Materials*, Vol. 383, pp 1-24, 2008.

[11] Degenhardt R, Bethge A, Rohwer K, Zimmermann R, Kling A, Tessmer J and Calvi A. Probabilistic approach for an improved buckling knock-down factors of CFRP cylindrical shells. Proceedings of the *1st European Air and Space Conference (CEAS)*, Berlin, Germany, 10-13 September, 2007.

[12] Orifici A, Thomson RS, Degenhardt R, Kling A, Rohwer K and Bayandor J. Degradation investigation in a postbuckling composite stiffened fuselage panel. *13th International Conference of Composite Structures*, Melbourne, Australia, 14-16 November, 2005.

[13] Geier B and Singh G. Some simple solution for buckling loads of thin and moderately thick cylindrical shells and panels made of laminated composite material. *Aerospace Science and Technology*, Vol. 1, pp 47-63, 1997.

[14] Bürmann P, Rolfes R, Tessmer Jand Schagerl M. A semi-analytical model for local post-buckling analysis of stringer- and frame-stiffened cylindrical panels. *Thin-Walled Structures*, Vol. 44, pp 102-114, 2006.

[15] Roache PJ. *Verification and Validation in Computational Science and Engineering*, Hermosa Publisher, 1998.

[16] Kling A, Tessmer J and Degenhardt R. Validation Procedure for Nonlinear Analysis of Stringer Stiffened CFRP Panels. *Proceedings of the 25th Congress of International Council of the Aeronautical Sciences*, Hamburg, Germany, 3-8 September, 2006.

Copyright Statement